

## Low Carbon Content NiTi Shape Memory Alloy Produced by Electron Beam Melting

*Jorge Otubo<sup>a,b,\*</sup>, Odair Doná Rigo<sup>b</sup>, Carlos de Moura Neto<sup>a</sup>,  
Michael Joseph Kaufman<sup>c</sup>, Paulo Roberto Mei<sup>b</sup>*

<sup>a</sup>*Instituto Tecnológico de Aeronáutica - CTA, 12228-900, S. J. dos Campos - SP, Brazil*

<sup>b</sup>*DEMA/FEM/UNICAMP, 13083-970, Campinas - SP, Brazil*

<sup>c</sup>*MSE - University of Florida, 32611, Gainesville - FL, USA*

Received: July 30, 2003; Revised: October 21, 2003

Earlier works showed that the use of electron beam melting is a viable process to produce NiTi shape memory alloy. In those works a static and a semi-dynamic processes were used producing small shell-shaped and cylindrical ingots respectively. The main characteristics of those samples were low carbon concentration and good composition homogeneity throughout the samples. This paper presents the results of scaling up the ingot size and processing procedure using continuous charge feeding and continuous casting. The composition homogeneity was very good demonstrated by small variation in martensitic transformation temperatures with carbon content around 0.013wt% compared to 0.04 to 0.06wt% of commercial products.

**Keywords:** *NiTi, Shape Memory, Electron Beam Melting, Martensitic Transformation*

### 1. Introduction

The usual process to produce NiTi shape memory alloys (hereafter called NiTi SMA) is by Vacuum Induction Melting (VIM) using high-density graphite crucibles to minimize the carbon contamination of the melt. Carbon combines with titanium precipitating TiC particles resulting in an alloy matrix richer in nickel content than the nominal composition consequently lowering the martensitic transformation temperatures<sup>1,2</sup>.

An alternative to VIM is the electron beam melting (EBM) to produce NiTi SMA. This process is known since the 1950's for refining refractory metals such as Mo, Ta, Nb and W and also reactive metals such as Ti, Zr, Hf and its alloys<sup>3</sup>. More recently this process has been used to produce alloys such as Ti6Al4V<sup>4,5,6</sup> and very clean superalloys<sup>7</sup>. On the other hand, its use to produce NiTi SMA is uncommon. Beside this author group, which has been working on the development of the EBM process to produce NiTi SMA since 1997<sup>2,8</sup>, only Matsumoto produced some small samples in 1991<sup>9,10</sup>.

By using EBM, the carbon contamination is completely eliminated due to melting in a water-cooled copper crucible, and oxygen contamination is minimized due to operation in high vacuum (better than  $10^{-2}$  Pa). Therefore, the

carbon and oxygen contents in the final product depend mainly on their levels in the initial raw material. One of the disadvantages of working in high vacuum during melting and remelting is the difficulty of controlling the nominal chemical composition due to some component evaporation changing the martensitic transformation temperatures, especially on the nickel-rich side of the phase diagram<sup>1,2</sup>. There are basically three possibilities of melting and casting using the 80 kW EB furnace used in this work: The first one is a static process where the elements (nickel plus titanium) are charged at once with desired nominal composition onto water cooled copper crucible that serves also as the casting mold. Using this process, it is possible to produce samples from a few grams up to a maximum of 350 g limited by the EB power required to melt the charge and also by the loss of composition homogeneity. The second one is a semi-dynamic process where the raw materials are continuously fed and cast into constant volume cylindrical water-cooled copper mold. Here the limitation is the mold height that cannot be too large, being its maximum around 50 mm. Larger axial height of the mold promotes differential EB incidence being lower when the melt pool level is at the bottom then gradually increasing as the pool level rises as the melting

\*e-mail: jotubo@ita.br

proceeds. Consequently, there are axial composition changes resulting in martensitic transformation temperature variations. The maximum weight that can be cast by this process is around 500 g. These two processes were already tested and the results were published elsewhere and the carbon content in the final products was very low and ranged from 0.007 to 0.016 wt% compared to 0.04 to 0.06 wt% for VIM processed ingots<sup>2,8</sup>. The third process whose results are presented in this work is a dynamic process with continuous feeding and continuous ingot casting overcoming the above limitations and scaling up the size and weight of the ingots.

## 2. Experimental Procedure

The Figure 1 shows the EB furnace, model EMO 80 with 80 kW EB power used in this work to produce NiTi SMA ingots. In a dynamic process the raw material (nickel + titanium) is laterally fed continuously by the feeding mechanism (A – feeding mechanism) into the path of a vertical electron beam that melts the charge (B – melting chamber). Simultaneously the melted product drops onto water-cooled copper extractor that is mounted inside the water-cooled copper mold resulting in ingots with maximum length of 800 mm.

The nickel used in this work was also produced by the above mentioned dynamic process casting 50 mm in diameter ingot. This ingot was machined to 45 mm in diameter to remove the surface defects, heated to 950 °C and hot rolled to 18 mm in diameter round bar. From 18 mm in diameter, the bar was cold rolled down to 4 × 4 mm<sup>2</sup> square rod (Fig. 2a). For this work it was used 18 pieces of 0.41 × 35 × 975 mm<sup>3</sup> grade 1 titanium sheets (Fig. 2b) imported from Kobe Steel plus 9 nickel bars of 4 × 4 × 975 mm<sup>3</sup>. The nickel bars and titanium sheets were intercalated with each other and then

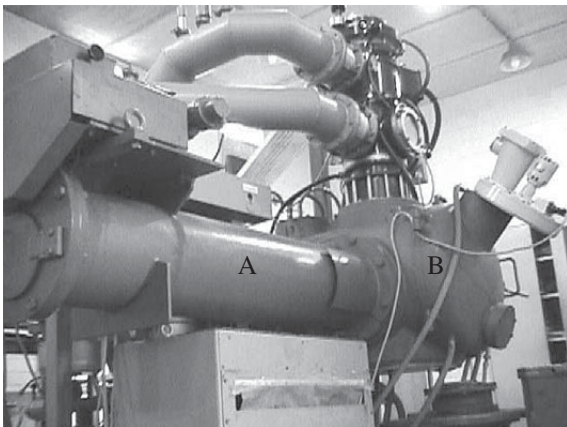


**Figure 1.** EB furnace, model EMO 80, with 80 kW EB power. A – Lateral feeding mechanism and B – Melting chamber.

encased inside a two U shaped titanium boxes resulting in a feeding bar of 35 × 35 × 975 mm<sup>3</sup> (Fig. 2c). The set was consolidated by TIG welding (Fig. 2d). The feeding charge nominal composition along the length was 54.7wt%Ni. The EB power used was 6.5 kW with a melting chamber internal pressure of 2 to 4 × 10<sup>-3</sup> Pa. For casting it was used a 40 mm diameter copper mold. During melting and casting it was observed that the dimensions of the feeding bar of 35 × 35 mm<sup>2</sup> was not adequate for the 40 mm diameter copper mold. Any small misalignment of the feeding bar promoted dripping off the liquid outside the mold. In order to avoid this problem, the feeding bar configuration was changed to a 25 × 40 mm<sup>2</sup> rectangular bar positioning the thinner side normal to the incident beam direction. The second charge was cast over the first ingot and then, remelted twice to improve the surface quality.

## 3. Results and Discussions

The upper part of Fig. 3 presents the 40 mm in diameter by 300 mm long ingot weighing around 2.5 kg after first casting. Some surface oxidation, cold junctions and also some cracks can be seen. In order to eliminate these surface defects, the ingot was remelted twice and it is shown in the lower part of Fig. 3. The remelted ingot also contains some surface defects mainly near the right end which corresponds to the ingot bottom where solidification starts. The surface defects disappear when the melting and casting process ac-

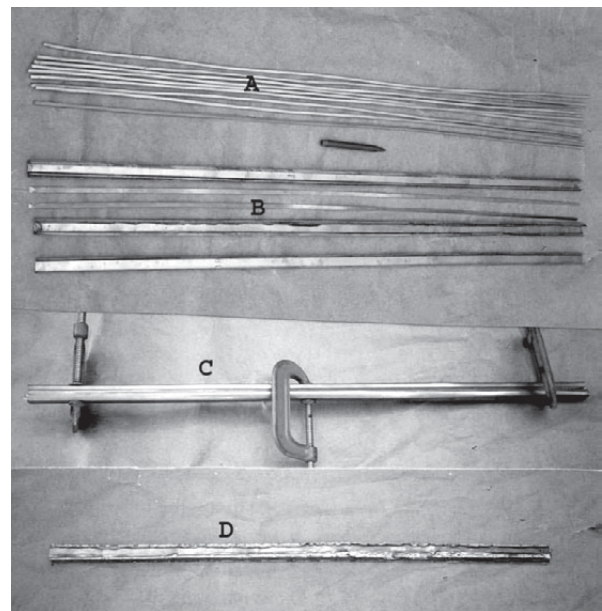


**Figure 2.** Mounting sequence of feeding charge: A – nickel bars; B – titanium sheets; C – Ni+Ti assembled for welding; and D – TIG welded charge.

quires a dynamic stationary equilibrium. After one melting and two remeltings, the final ingot weight was 2.2 kg with 40 mm diameter by 270 mm long. To check the chemical composition homogeneity, samples were taken from the bottom and top of the ingot after removing about 5 mm from both ends. Then from each end, three samples were taken going through radial direction as follows: one from the center (TC or BC), one from the middle radius (TMR or BMR) and one from near the border (TB or BB). T is for Top position and B for Bottom position of the ingot.

The ingot homogeneity was checked analyzing the direct and reverse martensitic transformation temperatures from DSC measurements as shown in Table 1. The oxygen and carbon content is also shown in Table 1. The results were analyzed in terms of  $M_p$  and  $A_p$ , which are the peak temperatures of the direct and reverse martensitic transformations. These parameters are used to avoid misinterpretation of the results which usually occurs when one uses the starting and finishing direct and reverse martensitic trans-

formations temperature,  $M_s$ ,  $M_f$ ,  $A_s$  and  $A_f$  respectively. In spite of this fact the results are shown in Table 1 in order to make possible comparison to data shown in the literature. Starting from ingot top position, we can see that both peak temperatures presented very small variation of 2 °C for  $M_p$  and 1.6 °C for  $A_p$  denoting good radial homogeneity. Now for ingot bottom position after discarding 5 mm, the difference on  $M_p$  data is 6 °C and on  $A_p$  is 3.4 °C indicating that dynamic stationary equilibrium had not been achieved up to this height. Now if we compare the average values of peak temperatures between the bottom and top of the ingot, the difference is around 1 °C which is very encouraging. That is, the ingot presented very good composition homogeneity along both radial and axial directions. This aspect can be seen clearly in Fig. 4 where  $M_p$  and  $A_p$  values are plotted for both positions. Although in terms of operational aspect is much more difficulty to control the dynamic process of continuous feeding and continuous ingot extraction, once the stationary equilibrium is reached, the result of fi-

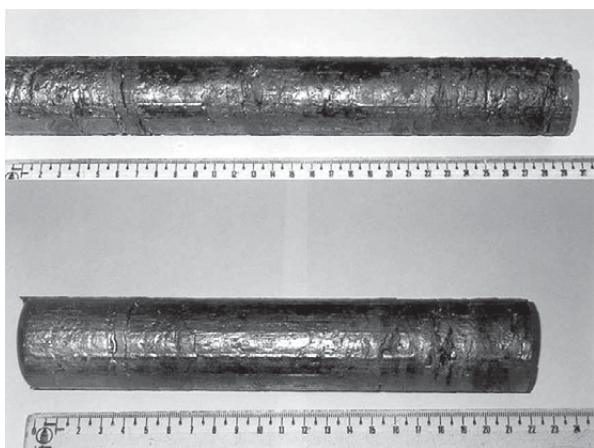


**Figure 3.** EBM ingot: upper, after first melting; lower, after two remelting.

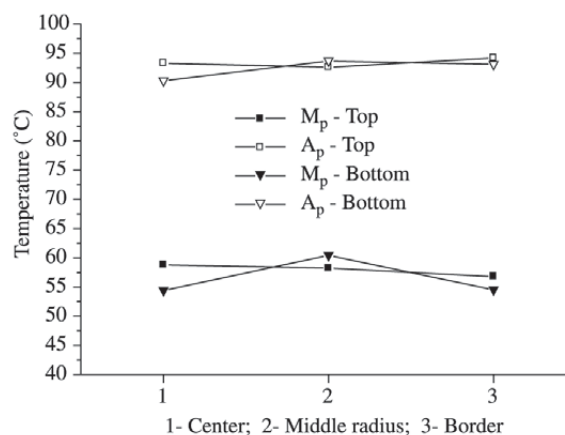


**Figure 4.** Direct and reverse peak martensitic transformation temperatures,  $M_p$  and  $A_p$  as a function of radial direction at ingot top position and bottom position.

**Table 1.** Direct and reverse martensitic transformation temperatures of EBM and VIM processed ingots.

Sample	wt%Ni (nom.)	wt%C	wt%O	$M_f$ (°C)	$M_p$ (°C)	$M_s$ (°C)	$A_s$ (°C)	$A_p$ (°C)	$A_f$ (°C)
TC	54.7	0.013	0.064	51.0	58.8	65.1	78.9	93.3	97.6
TMR				49.7	58.2	65.6	77.0	92.6	97.9
TB				49.0	56.8	65.0	79.5	94.2	99.1
BC				45.8	54.4	63.7	77.3	90.3	97.5
BMR				54.3	60.4	65.7	81.9	93.7	97.5
BB				48.0	56.1	65.4	79.5	93.1	99.9
VIM-1	55.5	0.058	0.0837	-13.8	-1.4	5.0	6.0	17.8	25.6

nal ingot in terms of chemical composition uniformity is superior when compared do semi-dynamic process of continuous feeding and static casting<sup>10</sup>. Besides that the scaling up is only possible in dynamic process. With EMO 80 used in this work it is possible to produce ingot of 800 mm long with 100 mm diameter.

Another aspect that should be emphasized is the low values of carbon content, 0.013wt%, that was presented by EBM processed ingot compared to about 0.06wt% of VIM product, that is, almost five times lower. This aspect could be seen very clearly from micrographies. Figure 5a shows the micrography of EBM ingot and no TiC particles is seen as far as the carbon

content is lower than the solubility limit of 0.025wt%. Figure 5b is from VIM ingot which contains 0.058wt% of carbon showing the orange colored TiC particles.

This work confirms the earlier results<sup>2,8</sup> showing that the use of EBM process to produce NiTi SMA is perfectly viable and that the use of dynamic process for scaling up is also possible. The researches are in progress to analyze operational aspects of EBM to scale up the process. The possibilities to produce much clean material than ever made certainly will be important in areas such as medical application opening new possibilities. Also the possibilities of producing clean material with low carbon content open the necessity to reanalyze data such as martensitic transformation temperatures, pseudoelasticity and other shape memory properties and mainly corrosion resistance that certainly should be improved by the high purity material.

#### 4. Conclusions

It has been shown that electron beam melting can be scaled up to produce relatively large ingots of NiTi shape memory alloys. The specific conclusions from this work are summarized below.

By dynamic process of continuous charge feeding and continuous casting it was produced a 270 mm long by 40 mm in diameter ingot weighing around 2.2 kg after one melting and two remelting.

The radial homogeneity was very good confirmed by small variation of around 2 and 6 °C in peak martensitic transformation temperatures for the top position and bottom position respectively.

The homogeneity along the length was also very good with the average of peak temperature difference of only 1 °C.

The carbon content of EBM ingot was 0.013wt% that is almost five times lower than the values presented by VIM processed ingot.

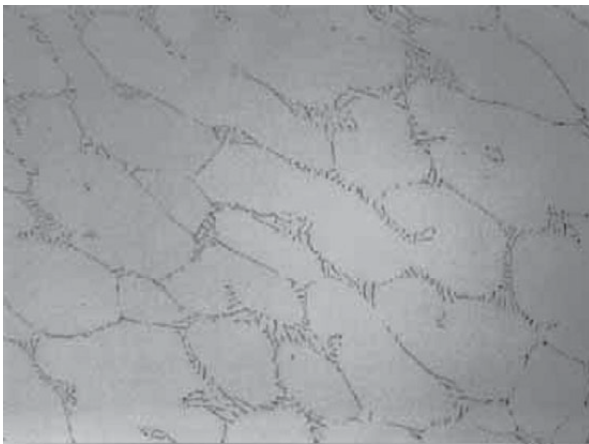
The oxygen content depends upon the raw material as far as the melting chamber internal pressure is very low ( $10^{-3}$  to  $10^{-2}$  Pa).

#### Acknowledgements

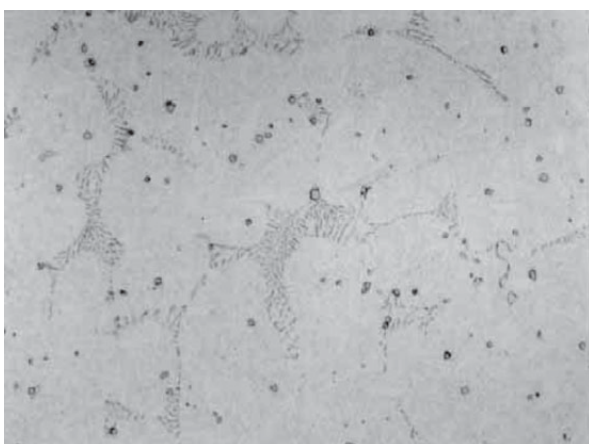
To FAPESP (grants 98/10971-1; 99/06399-3 and 00/09730-1); AEB (grant 2053); CNPq, Villares Metals; IPEN; UNICAMP; INPE; ITA/CTA and NSF for supporting this project.

#### References

1. Bellen, P.; Kumar, K.C.H.; Wollants, P.Z. *Z. Metallkd.*, v. 87, p. 972-978, 1996.
2. Otubo, J.; Mei, P.R.; Koshimizu, S.; Martinez, L.G. *The Third Pacific Rim International Conference on Advanced Materials and Processing - PRICM-3*, July 12-16, 1998,



a)



b)

**Figure 5.** a) TiC precipitates free EBM ingot, 0.013wt%C (400X); b) Orange colored TiC precipitates from VIM ingot, 0.058wt%C (200X). Etchant: 85v%H<sub>2</sub>O + 10v%HNO<sub>3</sub> + 5v%HF.



- Honolulu, Hawaii, USA, v. 1, p. 1063-1068, Edited by M. A. Imam, R. DeNale, S. Hanada, Z. Zhong and D. N. Lee, published by The Minerals, Metals & Materials Society, TMS.
3. Winkler, O.; Bakish, R. *Vacuum Metallurgy*, chapter 4, Elsevier Publishing Company, 1971.
  4. Choudhury, A. *ISIJ International*, v. 32, p. 563-554, 1992.
  5. Nakayma, T.; Kuroda, A.; Kurita, K. *ISIJ International*, v. 32, p. 583-592, 1992.
  6. Watanabe, S.; Suzuki, K.; Nishikawa, K. *ISIJ International*, v. 32, p. 625-629, 1992.
  7. Mitchell, A. *ISIJ International*, v. 32, p. 557-562, 1992.
  8. Otubo, J.; Rigo, O.D.; Moura Neto, C.; Kaufman, M.J.; Mei, P.R. *International Conference on Martensitic Transformation, ICOMAT'02*, Espoo, Finland, 09-13 June 2002. To be published in *Journal de Physique IV*.
  9. Matsumoto, H. *Journal of Materials Science Letters*, v. 10, p. 417-419, 1991.
  10. Matsumoto, H. *Journal of Materials Science Letters*, v. 10, p. 596-597, 1991.

